

# Photo-Induced State Conversion Mechanism of an Optically Durable Molecular Memory with Controlled Hydrogen Bonding: A Spin–Orbit CI Study of $[\{\text{Co}(\text{Hbim})(\text{C}_6\text{H}_4\text{O}_2)(\text{NH}_3)_2\}_2]$

Hirotohi Mori<sup>\*,†</sup> and Eisaku Miyoshi

Graduate School of Engineering Sciences, Kyushu University, 6-1 Kasuga Park, Fukuoka 816-8580

Received April 25, 2007; E-mail: miyoshi@asem.kyushu-u.ac.jp

The possibility for photon-mode memory writing of  $[\{\text{Co}(\text{Hbim})(\text{C}_6\text{H}_4\text{O}_2)(\text{NH}_3)_2\}_2]$  (Hbim = 2,2′-biimidazole) is examined from results obtained by spin–orbit complete active space configuration interaction (SO-CASCI) calculations. The spin-crossover phenomenon in the proton–electron-coupled complex monomer  $[\text{Co}(\text{Hbim})(\text{C}_6\text{H}_4\text{O}_2)(\text{NH}_3)_2]$  is a key process in memory writing to the complex dimer. We found a possibility of an efficient spin-crossover in the monomer. UV (ca. 300 nm) irradiation of the monomer  $^1\text{A}'$  state leads to a spin-crossover into the high-spin  $^5\text{A}'$  state. The back photoreaction from the  $^5\text{A}'$  to  $^1\text{A}'$  state is also possible with vis (ca. 600–700 nm) excitation. In these spin-crossover and back spin-crossover reactions, the intermediate triplet states,  $1^3\text{A}''$  and  $2^3\text{A}''$ , are found to participate.

The development of molecular memory is one of a number of exciting and hot fields in photochemistry and nanotechnology. In recent years, many scientists have tried to fabricate molecular memory with photochromic molecules, e.g. diarylethene,<sup>1–4</sup> azobenzene,<sup>5–8</sup> spiropyran,<sup>9</sup> and fulgide<sup>10,11</sup> derivatives, since these molecules show a digital response to photons and are considered to be suitable for generating bistable electronic states. These electronic states are required to generate the on–off switching states in molecular memory. In particular, diarylethene derivatives have been successful in controlling digital switching by irradiation with ultraviolet (UV) and visible (vis) light and are expected to function as erasable media.<sup>1</sup>

Unfortunately, however, the photon mode memories of these organic molecules are difficult to protect. That is, once the molecular memories have been read with UV (or vis) light, they may be erased due to probe-light-induced photochromic reactions. This problem is referred to as “memory degradation in photon mode memory,” and is a serious setback to the construction of reliable molecular memory. Thus, there has been a strong demand for developing new memory-molecules and appropriate techniques to read its photon-mode memory without undergoing degradation.

Recently, from a quantum chemical point of view, we have introduced a new class of molecular memory: proton–electron-coupled molecular memory, whose memory can be read without a UV–vis probe.<sup>12–14</sup> In these studies, the inorganic complex dimer  $[\{\text{Co}(\text{Hbim})(\text{C}_6\text{H}_4\text{O}_2)(\text{NH}_3)_2\}_2]$  (Hbim = 2,2′-biimidazole) (see Fig. 1) has been proposed as a candidate for such proton–electron-coupled molecular memory, which have three stable energy minima in  $^1\text{A}_g$ ,  $^5\text{A}_1$ , and  $^9\text{A}_g$  states. An indirect memory reading technique using IR probe light, which can be established only with proton–electron-coupled inorganic complexes, was also proposed in the studies<sup>12,13</sup>

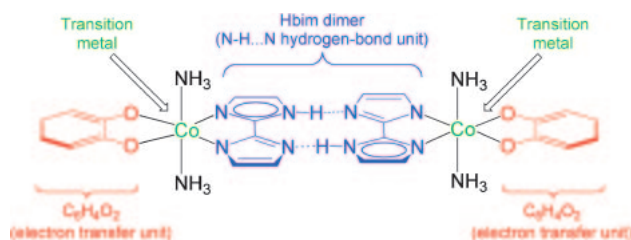


Fig. 1. The chemical structure of our introduced molecular memory: proton–electron-coupled molecular memory. By combining hydrogen-bonded unit (Hbim) and electron-transfer unit ( $\text{C}_6\text{H}_4\text{O}_2$ ), it could be possible to couple the motion of proton with the electron's in the complex.

and low-lying excited electronic states in the multistable energy minima were investigated.<sup>14</sup> In the middle-spin  $^5\text{A}_1$  state proton-transfer was observed, resulting in the red-shift of major N–H vibrational stretching in a theoretical IR spectrum.<sup>14</sup> In this paper, we will discuss the possibility and methods for writing (and re-writing) molecular memory of the proton–electron-coupled inorganic complex dimer  $[\{\text{Co}(\text{Hbim})(\text{C}_6\text{H}_4\text{O}_2)(\text{NH}_3)_2\}_2]$ .

## Theoretical Design of Proton–Electron-Coupled Molecular Memory

As mentioned in the previous section, an indirect electronic state detection method without UV–vis electronic excitation is an optimal way to read photon mode molecular memory in a stable manner. Establishing a means to avoid direct molecular memory detection with UV–vis excitation is in question.

The essence of optically durable molecular memory reading is to read the memories without experiencing any change of their electronic states. If we can use low-energy IR photon as a memory probe, we can construct an optically durable molecular memory system. From the above requirement, we reached the idea of a proton–electron-coupled system with

<sup>†</sup> Present address: Department of Chemistry, Iowa State University, Ames, Iowa 50011, USA

controlled hydrogen bonds.<sup>12,13</sup> As is widely known, the strength of a hydrogen bond can be determined from IR spectra. Moreover, since the strength of a hydrogen bond depends on the electronic environment around it, it is possible to control the IR spectral pattern if the motions of the proton and electron can be coupled in a single molecule. It was not difficult to imagine that such a proton–electron coupling is achieved in a mixed-valence inorganic complex linked with complementary hydrogen bonds, since the introduction of the transition metal (Ni) into the hydrogen-bonded inorganic complex polymer  $[\text{Ni}^{\text{II}}(2,2'\text{-biimidazolate}^-)_2]$  causes the formation of very strong hydrogen bonds.<sup>15–17</sup> Thus, we tried to find a hydrogen-bonded complex dimer having multi-stable electronic states, and finally reached the hydrogen-bonded complex dimer  $[\{\text{Co}(\text{Hbim})(\text{C}_6\text{H}_4\text{O}_2)(\text{NH}_3)_2\}_2]$ .<sup>12,13</sup>

An important point in our design of optically durable molecular memory is the installation of the redox-active ligand *o*-benzoquinone (bq). Since the frontier  $\pi$  orbital of bq is very close to the Co  $3d_\gamma$  orbital in energy, bq binds to the cobalt ion to form bistable electronic states with intramolecular charge transfer;  $\text{Co}^{\text{III}}\text{--cat}^{2-} \leftrightarrow \text{Co}^{\text{I}}\text{--bq}$ ,  $\text{cat}^{2-}$  is the two-electron-reduced form of bq).<sup>18–21</sup> Combining with the intramolecular redox function of bq and hydrogen-bonding function of Hbim, we have succeeded in theoretically showing the existence of controlled hydrogen bonds in the hydrogen-bonded inorganic complex dimer  $[\{\text{Co}(\text{Hbim})(\text{C}_6\text{H}_4\text{O}_2)(\text{NH}_3)_2\}_2]$ .<sup>12,13</sup> In other words, coupling of the motions of proton and electron is established in the complex, and the multi-stable electronic states of the complex dimer can be distinguished but with an IR probe light. Thus, we can use the complex dimer as an optically durable molecular memory.

### Computational Details

As mentioned above, it has been previously confirmed that the proton–electron-coupled inorganic complex dimer  $[\{\text{Co}(\text{Hbim})(\text{C}_6\text{H}_4\text{O}_2)(\text{NH}_3)_2\}_2]$  has three energy minima in the  $^1\text{A}_g$ ,  $^5\text{A}_1$ , and  $^9\text{A}_g$  states, respectively. To search the possibility and appropriate method for photo-induced memory writing (or re-writing) of the complex, a theoretical study for the electronic excited states of the complex dimer has been recommended.

If we want to use multi-stable electronic states whose spin multiplicity is different from each other as a molecular level memory-bit, the light-induced excited spin state trapping (LIESST) process, which is generally spin-forbidden, should be allowed. As is well known, the spin–orbit interaction plays an important role in a smooth LIESST process.<sup>22–26</sup> Thus, second, we performed spin–orbit complete active space configuration interaction (SO-CASCI) calculations to obtain the spin–orbit coupling (SOC) values between the different spin-states, which indicate the easiness of the generally forbidden LIESST transition. Since the difference between the three stable electronic states,  $^1\text{A}_g$ ,  $^5\text{A}_1$ , and  $^9\text{A}_g$ , of the hydrogen-bonded complex dimer  $[\{\text{Co}(\text{Hbim})(\text{C}_6\text{H}_4\text{O}_2)(\text{NH}_3)_2\}_2]$  comes from the electronic state conversion of a constituent complex monomer  $[\text{Co}(\text{Hbim})(\text{C}_6\text{H}_4\text{O}_2)(\text{NH}_3)_2]$  loosely bound by hydrogen-bonding interactions, as shown in the previous study,<sup>14</sup> we used a complex monomer model in the SO-CASCI calculations.

Reference wave functions used in these SO-CASCI calculations were obtained from preliminary CASSCF (12,9) calculations. The active orbitals comprised the five  $d$  orbitals of the cobalt ion center and a pair of  $\pi$  and  $\pi^*$  orbitals corresponding to Hbim ( $\text{H}_2\text{bim}$ , bim) and bq ( $\text{cat}^{2-}$ ), which were carefully chosen to express the low-lying excited states of the complex monomer  $[\text{Co}(\text{Hbim})(\text{C}_6\text{H}_4\text{O}_2)(\text{NH}_3)_2]$ . The active orbitals are shown in Fig. 2. Using the CASSCF (14,10) wave function and full Breit-Pauli Hamiltonian,<sup>27</sup> it was possible to diagonalize the spin–orbit CI matrix. The electronic configurations obtained using the SO-CASCI calculations are summarized in Table 1. From the obtained SOC values, we examined the possibility of the smooth LIESST process, that is, smooth memory writing process on the proton–electron-coupled complex. The GAMESS program package<sup>28</sup> was used for the SO-CASCI calculations.

The basis sets used in all calculations in this work were SBKJVC VDZ ECP for the Co atoms<sup>29</sup> and 6-31G(d,p) for the other (H, C, N, and O) atoms.<sup>30</sup>

### Results and Discussion

Here, we will discuss the excited state dynamics after the electronic excitation and writing process of proton–electron-coupled molecular memory. As we mentioned in the Computational Details section, the spin-state conversion of the hydrogen-bonded complex dimer  $[\{\text{Co}(\text{Hbim})(\text{C}_6\text{H}_4\text{O}_2)(\text{NH}_3)_2\}_2]$  basically comes from the spin-state conversions of the complex monomer  $[\text{Co}(\text{Hbim})(\text{C}_6\text{H}_4\text{O}_2)(\text{NH}_3)_2]$ , which constitutes the complex dimer. Figure 3 shows the difference in the spin densities of the  $^5\text{A}_1$  and  $^9\text{A}_g$  states, indicating that the  $^9\text{A}_g$  state of the monomers consists of two local quintet states. Therefore, we can reduce the problem of the excited states for the hydrogen-bonded dimer  $[\{\text{Co}(\text{Hbim})(\text{C}_6\text{H}_4\text{O}_2)(\text{NH}_3)_2\}_2]$  to a problem of the monomer  $[\text{Co}(\text{Hbim})(\text{C}_6\text{H}_4\text{O}_2)(\text{NH}_3)_2]$ . The spin-state conversion  $^1\text{A}_g \rightleftharpoons ^5\text{A}_1 \rightleftharpoons ^9\text{A}_g$  in the dimer complex  $[\{\text{Co}(\text{Hbim})(\text{C}_6\text{H}_4\text{O}_2)(\text{NH}_3)_2\}_2]$  can be approximated to a combination of the spin-state conversions  $^1\text{A}' \rightleftharpoons ^5\text{A}'$  in the two monomer  $[\text{Co}(\text{Hbim})(\text{C}_6\text{H}_4\text{O}_2)(\text{NH}_3)_2]$  units. Thus, we discuss only the excited state spin-conversion dynamics of  $[\text{Co}(\text{Hbim})(\text{C}_6\text{H}_4\text{O}_2)(\text{NH}_3)_2]$ .

A schematic energy diagram of  $[\text{Co}(\text{Hbim})(\text{C}_6\text{H}_4\text{O}_2)(\text{NH}_3)_2]$  obtained using TD/B3LYP calculations is shown in Fig. 4. It is well known that spin-crossover complexes generally have a metastable state whose spin multiplicity is between those of the low- and high-spin states. As shown in Fig. 4, such an intermediate metastable triplet state ( $^3\text{A}''$ ) was found in the complex monomer  $[\text{Co}(\text{Hbim})(\text{C}_6\text{H}_4\text{O}_2)(\text{NH}_3)_2]$ . In the figure, the spin–orbit-coupling constants (SOC) values calculated at the optimized geometry of the initial  $^1\text{A}'$ ,  $^3\text{A}''$ , and  $^5\text{A}'$  states are also shown. The SO-CASCI calculations were also performed with B3LYP optimized geometry for both protonated  $[\text{Co}(\text{H}_2\text{bim})(\text{C}_6\text{H}_4\text{O}_2)(\text{NH}_3)_2]$  and deprotonated  $[\text{Co}(\text{bim})(\text{C}_6\text{H}_4\text{O}_2)(\text{NH}_3)_2]$  monomer units. Since the calculated SOC values for the protonated and deprotonated forms were similar to that of  $[\text{Co}(\text{Hbim})(\text{C}_6\text{H}_4\text{O}_2)(\text{NH}_3)_2]$ , we will discuss only the SOC values of the  $[\text{Co}(\text{Hbim})(\text{C}_6\text{H}_4\text{O}_2)(\text{NH}_3)_2]$ . Low-lying excited states of each spin-multiplicity calculated by TD/B3LYP and SO-CASCI calculations are qualitatively similar.

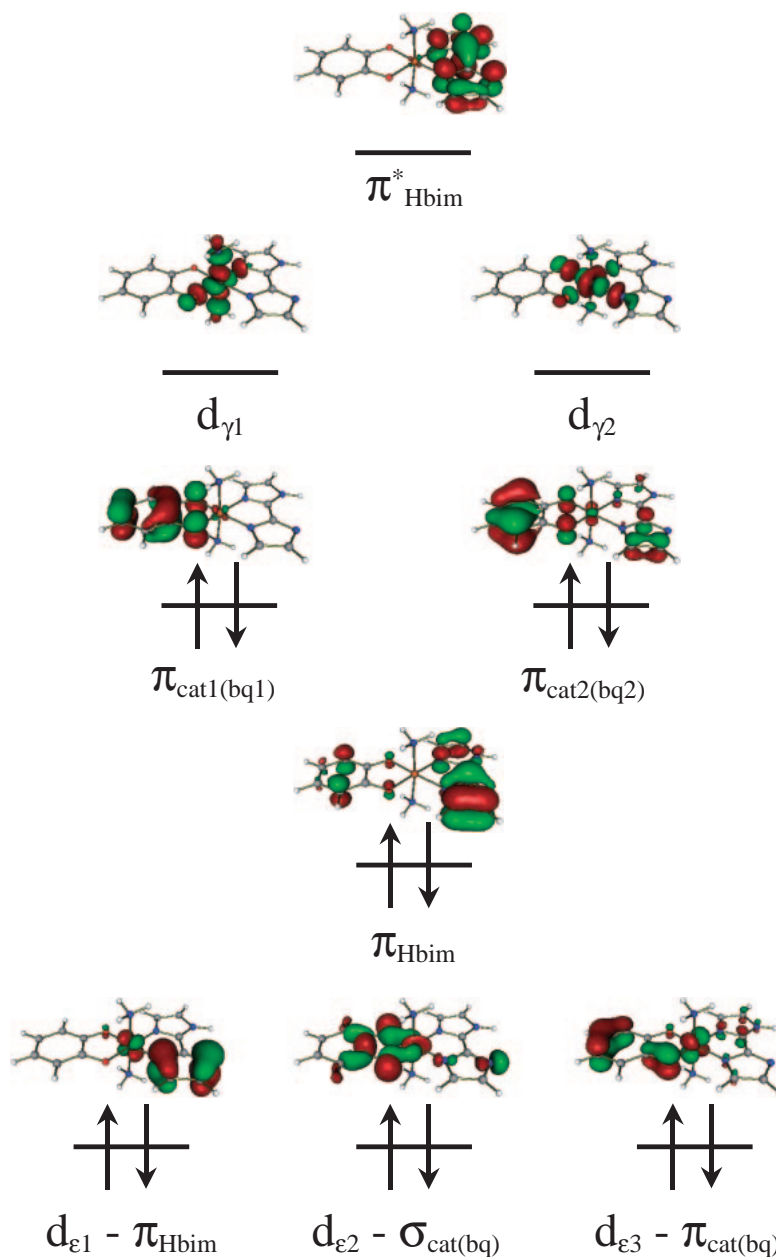


Fig. 2. The active orbitals used in the SO-CASCI (12,9) calculations. The electronic configuration of the ground  $^1A'$  state is shown.

Table 1. Electronic Configurations of  $[\text{Co}(\text{Hbim})(\text{C}_6\text{H}_4\text{O}_2)(\text{NH}_3)_2]$

Electronic states	Main electronic configurations	Label (symmetry)
Lowest singlet	$(\pi_{\text{Hbim}})^2(\pi_{\text{cat1}})^2(\pi_{\text{cat2}})^2(d_{\gamma 1})^0(d_{\gamma 2})^0$	$1^1A'$
First excited singlet	$(\pi_{\text{Hbim}})^2(\pi_{\text{cat1}})^2(\pi_{\text{cat2}})^1(d_{\gamma 1})^1(d_{\gamma 2})^0$	$1^1A''$
	$(\pi_{\text{Hbim}})^2(\pi_{\text{cat1}})^1(\pi_{\text{cat2}})^2(d_{\gamma 1})^1(d_{\gamma 2})^0$	
Lowest triplet <sup>a)</sup>	$(\pi_{\text{Hbim}})^2(\pi_{\text{sq1}})^2(\pi_{\text{sq2}})^1(d_{\gamma 1})^1(d_{\gamma 2})^0$	$1^3A''$
	$(\pi_{\text{Hbim}})^2(\pi_{\text{sq1}})^1(\pi_{\text{sq2}})^2(d_{\gamma 1})^1(d_{\gamma 2})^0$	
First excited triplet <sup>a)</sup>	$(\pi_{\text{Hbim}})^2(\pi_{\text{sq1}})^2(\pi_{\text{sq2}})^1(d_{\gamma 1})^0(d_{\gamma 2})^1$	$2^3A''$
	$(\pi_{\text{Hbim}})^2(\pi_{\text{sq1}})^1(\pi_{\text{sq2}})^2(d_{\gamma 1})^0(d_{\gamma 2})^1$	
Lowest quintet	$(\pi_{\text{Hbim}})^2(\pi_{\text{bq1}})^1(\pi_{\text{bq2}})^1(d_{\gamma 1})^1(d_{\gamma 2})^1$	$1^5A'$
First excited quintet	$(\pi_{\text{Hbim}})^1(\pi_{\text{bq1}})^2(\pi_{\text{bq2}})^1(d_{\gamma 1})^1(d_{\gamma 2})^1$	$2^5A'$
	$(\pi_{\text{Hbim}})^1(\pi_{\text{bq1}})^1(\pi_{\text{bq2}})^2(d_{\gamma 1})^1(d_{\gamma 2})^1$	

a) Semi-quinonate (sq) is the one-electron-reduced form of bq.

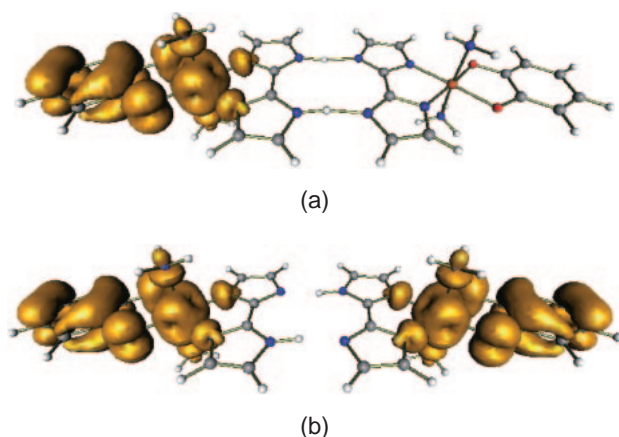


Fig. 3. Difference spin densities in (a) the  $^5A_1$  and (b)  $^9A_g$  states of the complex dimer  $[\text{Co}(\text{Hbim})(\text{C}_6\text{H}_4\text{O}_2)(\text{NH}_3)_2]_2$ .

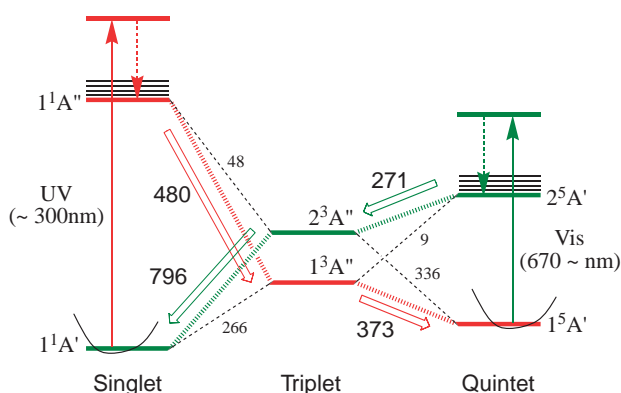


Fig. 4. Schematic energy diagram of  $[\text{Co}(\text{Hbim})(\text{C}_6\text{H}_4\text{O}_2)(\text{NH}_3)_2]$ . TD/B3LYP calculations were performed at the optimized structure of the lowest state of each spin-multiplicity. SOC constants between some spin states predicted by SO-CASCI calculations are shown along the dotted lines connecting those spin state energy levels. SO-CASCI calculations were performed at the optimized structure of spin-multiplicity of the initial state. The most probable photoreaction paths are indicated by colored lines (Red line: LIESST process,  $1^1A' \rightarrow 1^3A'' \rightarrow 1^5A'$ , Green line: back-LIESST process,  $1^5A' \rightarrow 2^3A'' \rightarrow 1^1A'$ ).

First, we focus on the photo-reaction path of the low-spin  $1^1A'$  state complex monomer  $[\text{Co}^{\text{III}}(\text{Hbim}^-)(\text{cat}^{2-})(\text{NH}_3)_2]$ . As was shown in the previous paper,<sup>14</sup>  $[\{\text{Co}^{\text{III}}(\text{Hbim}^-)(\text{cat}^{2-})(\text{NH}_3)_2\}_2]$  in the  $1^1A_g$  state has strong absorption peaks, which correspond to intra-ligand  $\pi-\pi^*$  excitations, in the UV region ( $<300\text{ nm}$ ). The TD/B3LYP calculations for the monomer  $[\text{Co}^{\text{III}}(\text{Hbim}^-)(\text{cat}^{2-})(\text{NH}_3)_2]$  unit in  $1^1A'$  also showed a similar spectral pattern to that of the dimer. There are some singlet excited states whose oscillator strength are very small or zero in the region ( $>300\text{ nm}$ ). Therefore, immediately after a  $\pi-\pi^*$  excitation using UV photons, the  $[\text{Co}^{\text{III}}(\text{Hbim}^-)(\text{cat}^{2-})(\text{NH}_3)_2]$  unit is deexcited into the first singlet excited state via internal conversion. After the internal conversion, the molecule is deexcited into the lowest triplet (intermediate) states through strong spin-orbit coupling,  $\text{SOC}(1^1A'' \rightarrow 1^3A'') = 480\text{ cm}^{-1}$ . It is noteworthy that the SOC value between the first

excited  $1^1A''$  state and the second  $3^3A''$  state ( $\text{SOC}(1^1A'' \rightarrow 2^3A'') = 48\text{ cm}^{-1}$ ) is a tenth of the SOC for  $1^1A'' \rightarrow 1^3A''$ . The next process corresponds to the further deexcitation from the metastable  $1^3A''$  state. There are two deactivation channels, one to the initial low-spin  $1^1A'$  state and a second to the high-spin  $1^5A'$  state. The question arises as to which is the dominant reaction channel. The corresponding SOC values for each channel are  $\text{SOC}(1^3A'' \rightarrow 1^1A') = 266\text{ cm}^{-1}$  and  $\text{SOC}(1^3A'' \rightarrow 1^5A') = 373\text{ cm}^{-1}$ . Judging from the magnitudes of these SOC values, the deactivation process into the high-spin  $1^5A'$  state is preferred to deactivation into the low-spin  $1^1A'$  state. The deactivation process to the high-spin  $1^5A'$  state might become more dominant by introducing effective functional groups into the complex. Thus, the UV excitation of the complex monomer in the low-spin  $1^1A'$  state induces an efficient spin-crossover to generate the complex  $[\text{Co}^{\text{I}}(\text{Hbim})(\text{bq})(\text{NH}_3)_2]$  in the high-spin  $1^5A'$  state.

Second, we consider the excited state dynamics after electronic excitation of the complex monomer  $[\text{Co}^{\text{I}}(\text{Hbim}^-)(\text{bq})(\text{NH}_3)_2]$  in the high-spin  $1^5A'$  state. As mentioned in the previous subsection, the high-spin hydrogen-bonded complex dimer  $[\{\text{Co}^{\text{I}}(\text{Hbim}^-)(\text{bq})(\text{NH}_3)_2\}_2]$  has strong MLCT absorptions in the visible-light region. Similar to the low-spin state, the TD/B3LYP result for the monomer unit gave almost the same spectral feature as the dimer case. Thus, for the discussion on the excited state dynamics of the dimer, it is considered enough to analyze that of the monomer. After the MLCT excitation ( $600\text{--}700\text{ nm}$ ), the complex monomer in the high-spin hydrogen-bonded complex dimer  $[\{\text{Co}^{\text{I}}(\text{Hbim}^-)(\text{bq})(\text{NH}_3)_2\}_2]$  is deactivated into the first excited quintet state,  $1^5A''$ . Then, the complex is further deexcited into triplet metastable states through spin-orbit coupling. As shown in Fig. 4,  $\text{SOC}(1^5A'' \rightarrow 1^3A'') = 9\text{ cm}^{-1}$  and  $\text{SOC}(1^5A'' \rightarrow 2^3A'') = 271\text{ cm}^{-1}$ . Thus, the intersystem crossing efficiently proceeds into not the first but the second triplet state. Since the  $2^3A''$  state is coupled more strongly with the low-spin  $1^1A'$  state ( $\text{SOC}: 796\text{ cm}^{-1}$ ) than with the high-spin  $1^5A'$  state ( $\text{SOC}: 336\text{ cm}^{-1}$ ), the complex in the  $2^3A''$  state is efficiently deactivated into the  $1^1A'$  state. Thus, the photo-excitation of the complex monomer in the high-spin  $1^5A'$  state induces an efficient spin-crossover to generate the complex in the low-spin  $1^1A'$  state.

The above discussion of the SOC values shows that efficient spin-crossover, i.e. efficient memory-writing would be achieved in the proton-electron-coupled inorganic complex dimer  $[\{\text{Co}(\text{Hbim})(\text{C}_6\text{H}_4\text{O}_2)(\text{NH}_3)_2\}_2]$ , which we have theoretically introduced.<sup>13</sup> As summarized in above section, we have introduced a method to detect the molecular level information of  $[\{\text{Co}(\text{Hbim})(\text{C}_6\text{H}_4\text{O}_2)(\text{NH}_3)_2\}_2]$  using IR absorption to avoid memory degradation. Combining the IR memory detection method with the UV memory writing method, it will be possible to achieve a new optically durable molecular memory system. A scheme for explaining the mechanisms of the optically durable molecular memory system with the proton-electron-coupled inorganic complex  $[\{\text{Co}(\text{Hbim})(\text{C}_6\text{H}_4\text{O}_2)(\text{NH}_3)_2\}_2]$  is shown in Fig. 5. At the top of the figure, the initial  $1^1A_g$  state of the hydrogen-bonded complex dimer  $[\{\text{Co}^{\text{III}}(\text{Hbim}^-)(\text{cat}^{2-})(\text{NH}_3)_2\}_2]$  is shown. If we use IR light whose wavelength is ca.  $2100\text{ cm}^{-1}$  as a memory probe light, no IR absorp-

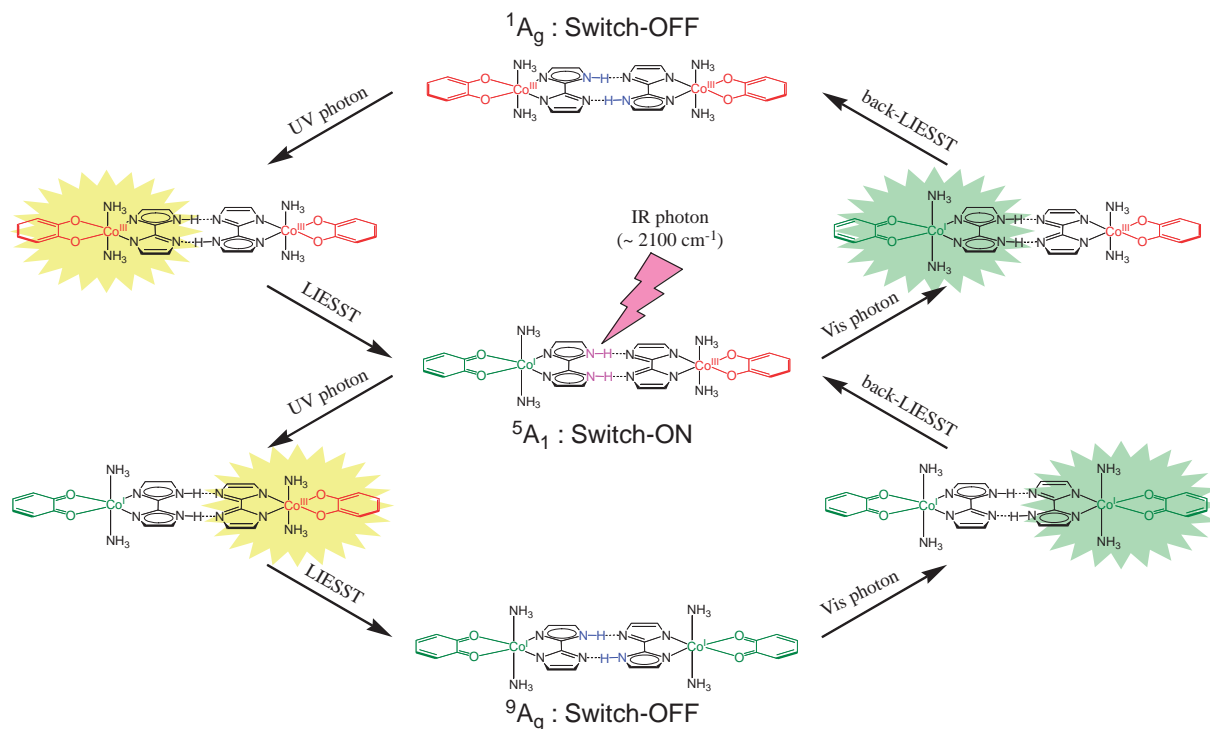


Fig. 5. Writing and reading of proton–electron-coupled molecular memory.

tion signal will be obtained in the  $^1A_g$  state.<sup>14</sup> Thus, we can define the  $^1A_g$  state as the “switch-OFF” state.

Since the width of the  $[\text{Co}(\text{Hbim})(\text{C}_6\text{H}_4\text{O}_2)(\text{NH}_3)_2]$  monomer unit is over 1 nm, it is considered possible that the monomer unit can be excited by using SNOM (Scanning Near-field Optical Microscopy) technique.<sup>31,32</sup> If one of the monomer  $[\text{Co}^{\text{III}}(\text{Hbim}^-)(\text{cat}^{2-})(\text{NH}_3)_2]$  units of  $[\{\text{Co}^{\text{III}}(\text{Hbim}^-)(\text{cat}^{2-})(\text{NH}_3)_2\}_2]$  in the  $^1A_g$  state is irradiated with UV photons, then we can generate the IR “switch-ON” state. The middle part of Fig. 5 reveals a schematic picture of the monomer after excitation. In the  $^1A_g$  state, the irradiated monomer unit is converted from the singlet ( $^1A'$ ) to the quintet spin state ( $^5A'$ ) through the strong SOC as mentioned above. Since the acidity of  $^5A'-[\text{Co}^{\text{I}}(\text{Hbim}^-)(\text{bq})(\text{NH}_3)_2]$  is larger than that of  $^1A'-[\text{Co}^{\text{III}}(\text{Hbim}^-)(\text{cat}^{2-})(\text{NH}_3)_2]$  immediately after the spin conversion, the NH proton of the  $^1A'$  monomer unit transfers to the second monomer to form the  $^1A'-[\text{Co}^{\text{III}}(\text{bim}^-)(\text{cat}^{2-})(\text{NH}_3)_2]$  and  $^5A'-[\text{Co}^{\text{I}}(\text{H}_2\text{bim}^-)(\text{bq})(\text{NH}_3)_2]$  units. Thus, we can generate a proton-transferred dimer complex  $^5A_1-[\text{Co}^{\text{III}}(\text{bim}^{2-})(\text{cat}^{2-})(\text{NH}_3)_2][\text{Co}^{\text{I}}(\text{H}_2\text{bim}^-)(\text{bq})(\text{NH}_3)_2]$  by using UV photo-excitation. In the  $^5A_1$  state, the probe IR light at around the 2100  $\text{cm}^{-1}$  energy region is strongly absorbed by the high-spin unit in the complex dimer. Thus, we can define the  $^5A_1$  state as the “switch-ON” state. It should be noted that the opposite operation, switch-ON  $\rightarrow$  switch-OFF, can be established by using a photon in the visible region. By irradiating the  $^5A'-[\text{Co}^{\text{I}}(\text{H}_2\text{bim}^-)(\text{bq})(\text{NH}_3)_2]$  high-spin monomer units in the dimer complex  $^5A_1-[\text{Co}^{\text{III}}(\text{bim}^{2-})(\text{cat}^{2-})(\text{NH}_3)_2][\text{Co}^{\text{I}}(\text{H}_2\text{bim}^-)(\text{bq})(\text{NH}_3)_2]$  with vis light (600–700 nm) using the SNOM technique, we can convert the  $^5A_1$  dimer complex back to the initial “switch-OFF”  $^1A'$  state.

If the low-spin monomer unit  $^1A'-[\text{Co}^{\text{III}}(\text{bim}^{2-})(\text{cat}^{2-})(\text{NH}_3)_2]$  is irradiated with UV light in the “switch-ON”  $^5A_1$

state, the question of what will happen arises. After the UV irradiation, the irradiated monomer unit is converted into the high-spin state. Thus, the total spin state of the dimer complex becomes a nonet state. Since the spin states of the two monomer units in the nonet state dimer complex are both quintets, the biased proton transferred to the  $[\text{Co}^{\text{III}}(\text{bim}^{2-})(\text{cat}^{2-})(\text{NH}_3)_2]$  unit in the  $^5A_1$  state is then transferred back to the initial position to form  $^9A_g-[\{\text{Co}^{\text{I}}(\text{Hbim}^-)(\text{bq})(\text{NH}_3)_2\}_2]$  (See Fig. 5). As a result, the generated state becomes the “switch-OFF” state. The behavior of the  $[\{\text{Co}^{\text{I}}(\text{Hbim}^-)(\text{bq})(\text{NH}_3)_2\}_2]$  to IR photons in the  $^9A_g$  state is similar to behavior of the dimer in the initial  $^1A_g$  state.

As explained above, it is possible to generate three stable electronic states in the  $[\{\text{Co}(\text{Hbim})(\text{C}_6\text{H}_4\text{O}_2)(\text{NH}_3)_2\}_2]$  complex dimer, and convert between them on irradiation with UV–vis light by using the spin–orbit-coupling feature in the complex. Furthermore, it is possible to distinguish between these three electronic states with an IR probe without changing the electronic states by using the proton–electron-coupling feature of the complex.

## Conclusion

The electronic excited states and photochemical reaction path of a proton–electron-coupled inorganic complex  $[\{\text{Co}(\text{Hbim})(\text{C}_6\text{H}_4\text{O}_2)(\text{NH}_3)_2\}_2]$ , which was previously designed for use as an optically durable IR-detectable molecular memory device, were theoretically studied using SO-CASCI calculations.

The evidence of the possibility for photon-mode memory writing of  $[\{\text{Co}(\text{Hbim})(\text{C}_6\text{H}_4\text{O}_2)(\text{NH}_3)_2\}_2]$  was also obtained. The spin-crossover phenomenon in the proton–electron-coupled complex monomer  $[\text{Co}(\text{Hbim})(\text{C}_6\text{H}_4\text{O}_2)(\text{NH}_3)_2]$  is a key process in memory writing on the hydrogen-bonded inorganic



complex dimer [ $\{\text{Co}(\text{Hbim})(\text{C}_6\text{H}_4\text{O}_2)(\text{NH}_3)_2\}_2$ ]. From the SO-CASCI results, we found possible evidence of an efficient spin-crossover process in  $[\text{Co}(\text{Hbim})(\text{C}_6\text{H}_4\text{O}_2)(\text{NH}_3)_2]$ . UV (ca. 300 nm) irradiation of the  $^1\text{A}'$  state monomer leads to a spin-crossover into the high-spin  $^5\text{A}'$  state. The back photo-reaction from the  $^5\text{A}'$  state to the  $^1\text{A}'$  state is also possible with Vis (ca. 600–700 nm) excitation. The intermediate triplet states which participate in these spin-crossover and back spin-crossover reactions are  $1^3\text{A}''$  and  $2^3\text{A}''$ . Since the intermediate triplet states are different in each reaction, direction selective photoreactions can be established. Thus, the SO-CASCI results predict the possibility of writing molecular-level memory with UV–vis electronic excitation in the proton–electron-coupled inorganic complex dimer [ $\{\text{Co}(\text{Hbim})(\text{C}_6\text{H}_4\text{O}_2)(\text{NH}_3)_2\}_2$ ].

The present study has been supported primarily by a Grant-in-Aid for Scientific Research from the Japan Society for the Promotion of Science (JSPS). The major part of the calculations reported here were performed using computing resources in the Research Center for Computational Science, Okazaki, Japan. HM is also grateful to JSPS for the Research Fellowships for Young Scientists.

## References

- 1 M. Irie, T. Fukaminato, T. Sasaki, N. Tamai, T. Kawai, *Nature* **2002**, 420, 759.
- 2 M. Irie, *Chem. Rev.* **2000**, 100, 1685.
- 3 H. Miyasaka, M. Murakami, A. Itaya, D. Guillaumont, S. Nakamura, M. Irie, *J. Am. Chem. Soc.* **2001**, 123, 753.
- 4 D. Guillaumont, T. Kobayashi, K. Kanda, H. Miyasaka, K. Uchida, S. Kobatake, K. Shibata, S. Nakamura, M. Irie, *J. Phys. Chem. A* **2002**, 106, 7222.
- 5 T. Yutaka, M. Kurihara, H. Nishihara, *Mol. Cryst. Liq. Cryst.* **2000**, 343, 193.
- 6 T. Yutaka, M. Kurihara, K. Kubo, H. Nishihara, *Inorg. Chem.* **2000**, 39, 3438.
- 7 T. Yutaka, I. Mori, M. Kurihara, J. Mizutani, K. Kubo, S. Furusho, K. Matsumura, N. Tamai, H. Nishihara, *Inorg. Chem.* **2001**, 40, 4986.
- 8 S. Kume, M. Kurihara, H. Nishihara, *Chem. Commun.* **2001**, 1656.
- 9 G. Berkovic, V. Krongauz, V. Weiss, *Chem. Rev.* **2000**, 100, 1741.
- 10 Y. Chen, C. Wang, M. Fan, B. Yao, N. Menke, *Opt. Mater.* **2004**, 26, 75.
- 11 M. Handschuh, M. Seibold, H. Port, H. C. Wolf, *J. Phys. Chem. A* **1997**, 101, 502.
- 12 H. Mori, E. Miyoshi, *Chem. Lett.* **2004**, 33, 758.
- 13 H. Mori, E. Miyoshi, *J. Theor. Comput. Chem.* **2005**, 4, 333.
- 14 H. Mori, E. Miyoshi, *Bull. Chem. Soc. Jpn.*, **2007**, 80, 1335.
- 15 H. Mori, E. Miyoshi, *Bull. Chem. Soc. Jpn.* **2004**, 77, 687.
- 16 M. Tadokoro, H. Kanno, T. Kitajima, H. Shimada-Umemoto, N. Nakanishi, K. Isobe, K. Nakasuji, *Proc. Natl. Acad. Sci. U.S.A.* **2002**, 99, 4950.
- 17 M. Tadokoro, K. Nakasuji, *Coord. Chem. Rev.* **2000**, 198, 205.
- 18 H.-C. Chang, S. Kitagawa, *Angew. Chem., Int. Ed.* **2002**, 41, 130.
- 19 C. G. Pierpont, *Coord. Chem. Rev.* **2001**, 216–217, 99.
- 20 D. M. Adams, L. Noodleman, D. N. Hendrickson, *Inorg. Chem.* **1997**, 36, 3966.
- 21 D. M. Adams, A. Dei, A. L. Rheingold, D. N. Hendrickson, *J. Am. Chem. Soc.* **1993**, 115, 8221.
- 22 O. Sato, *Acc. Chem. Res.* **2003**, 36, 692.
- 23 S. Decurtins, P. Gütllich, C. Köhler, H. P. Spiering, A. Hauser, *Chem. Phys. Lett.* **1984**, 105, 1.
- 24 P. Gütllich, A. Hauser, H. Spiering, *Angew. Chem., Int. Ed. Engl.* **1994**, 33, 2024.
- 25 P. Gütllich, Y. Garcia, H. A. Goodwin, *Chem. Soc. Rev.* **2000**, 29, 419.
- 26 M. Kondo, K. Yoshizawa, *Chem. Phys. Lett.* **2003**, 372, 519.
- 27 K. Balasubramanian, *Relativistic Effects in Chemistry Part A*, Wiley & Sons, New York, **1997**.
- 28 M. W. Schmidt, K. K. Baldrige, J. A. Boatz, S. T. Elbert, M. S. Gordon, J. H. Jensen, S. Koseki, N. Matsunaga, K. A. Nguyen, S. Su, T. L. Windus, M. Dupuis, J. A. Montgomery, *J. Comput. Chem.* **1993**, 14, 1347.
- 29 W. J. Stevens, M. Krauss, H. Basch, P. G. Jasien, *Can. J. Chem.* **1992**, 70, 612.
- 30 R. Ditchfield, W. J. Hehre, J. A. Pople, *J. Chem. Phys.* **1971**, 54, 724; W. J. Hehre, R. Ditchfield, J. A. Pople, *J. Chem. Phys.* **1972**, 56, 2257.
- 31 D. W. Pohl, W. Denk, M. Lanz, *Appl. Phys. Lett.* **1984**, 44, 651.
- 32 A. Lewis, M. Isaacson, A. Harootunian, A. Muray, *Ultramicroscopy* **1984**, 13, 227.